BMC Plant Biology

RESEARCH

Open Access

Transcriptomic analysis of peaches and nectarines reveals alternative mechanism for trichome formation

Chun-Che Huang[1†], Han-Wei Chen[1†], Jo-Wei Allison Hsieh[2,3†], Yen-Chun Lin[1], Yi-Pei Li[2], Chunxian Chen[4], Yen-Fang Song[5], Gung-Chian Yin[5], Te-Lun Mai[2], Ying-Chung Jimmy Lin[2,6,7*] and Yuan-Kai Tu[1*]

Abstract

Trichomes in *Prunus persica* (L.) Batsch are crucial specialized structures that play a protective role against both biotic and abiotic stresses. The fruits with and without trichomes are respectively named as peach and nectarine. At the genetic level, the formation of trichome in peach is controlled by a single gene, *PpMYB25*, at the *G* locus. Peach (*GG* or *Gg*) is dominant to nectarine (*gg*), but such regulatory role was reported in a small-scale accession. In this study, we performed large-scale genotype and phenotype screening on 295 accessions. Almost all accessions supported the casual relationship between trichome formation and *PpMYB25*. However, a peach to nectarine mutant, named Maravilha Nectarine Mutant (MN), was discovered to possess a putative functional *PpMYB25* gene sequence (*Gg*) but revealed nectarine phenotype. Comparative transcriptomic analyses revealed that *PpMYB25* transcript was absent in MN. Correlation analyses also demonstrated that the *PpMYB25*-mediated regulatory network was abolished in MN. In summary, our results demonstrated an alternative mechanism beyond genetic regulation on trichome formation.

Keywords *Prunus persica* (L.) Batsch, Transcriptome, Peach to nectarine mutant, Glabrous locus, MYB transcription factors, Differential gene expression

[†]Chun-Che Huang, Han-Wei Chen and Jo-Wei Allison Hsieh contributed equally to this work.

*Correspondence:
Ying-Chung Jimmy Lin
YCJimmyLin@ntu.edu.tw
Yuan-Kai Tu
yktu@tari.gov.tw
[1] Crop Genetic Resources and Biotechnology Division, Taiwan Agricultural Research Institute, Taichung 413008, Taiwan
[2] Department of Life Science, National Taiwan University, Taipei 10617, Taiwan
[3] The Genome Center, University of California, Davis, Davis, CA 95616, USA
[4] Southeastern Fruit and Tree Nut Research Laboratory, Agricultural Research Service, U.S. Department of Agriculture, 21 Dunbar Road, Byron, GA 31008, USA
[5] Experimental Facility Division, National Synchrotron Radiation Research Center, Hsinchu 30076, Taiwan
[6] Genome and Systems Biology Degree Program, National Taiwan University and Academia Sinica, Taipei 10617, Taiwan
[7] Institute of Plant Biology, National Taiwan University, Taipei 10617, Taiwan

Introduction

Trichomes in plants represent a type of specialized cells above the epidermal cells, primarily serving as an additional protective layer on the outermost surface for defense against both biotic and abiotic stresses [11]. For example, the pointed shape of trichomes prevent plants from insect or spider bites [33]. Clustering locations of trichomes form a protecting layer to buffer the mechanical stress caused from raindrops [16]. The trichomes may also serve as a "coat" to adapt to extremely environmental dynamics, such as the oscillation between wet and dry or cold and hot weathers [4, 12, 17], or protect plants from excessive UV light during development [31]. Thus, trichomes play a crucial role in ensuring survival of plants.

The initiation of trichome formation mainly is regulated by transcription factors, and there are two major different regulatory routes in plants. In *Arabidopsis*, trichome formation is initiated by a trimeric transcription factor (TF) complex, comprising R2R3 MYB, WD40 repeat, and basic helix-loop-helix (bHLH) proteins [13]. In cotton, *GhMYB25* initiates trichome formation, and the loss-of-function mutation in *GhMYB25* results in the absence of trichomes. Although *AtMYB106*, the homologous gene of *GhMYB25* in *Arabidopsis*, also participates in trichome formation, its mutant is still capable of forming trichomes. *AtMYB106* is not a required gene for trichome formation in *Arabidopsis* [15, 35, 36].

Peach, *Prunus persica* (L.) Batsch, can be regarded as a model plant in Rosaceae because of its relatively small genome size (~ 230 Mb) and short juvenility (~ 3 years to fruit) [1, 2]. Comparing to the genome of two well-known herbaceous (*Arabidopsis thaliana*, ~135 Mb) [21] and woody (*Populus trichocarpa*, ~500 Mb) [24] model plants in angiosperms, the genome size of *P. persica* appears to be highly suitable for comparative genomics and transcriptomics. Furthermore, the high-quality chromosome level assembly of peach reference genome [27] would minimize potential bias occurred during the bioinformatic analyses.

In addition to the small genome size and short reproductive cycle, many horticultural traits in peaches are found to be controlled by a single gene or locus, making peach an excellent plant species for studying the molecular mechanisms underlying traits. For example, the flat fruit trait in peaches is genetically controlled by a single gene, *PpOFP1*, or the "*S* locus" (saucer locus) localized on chromosome 6 [34]. *PpMYB10.1* is a master regulator of anthocyanin accumulation in red-skinned peach, which is at the *H* locus (highlighter locus) in chromosome 3 [23]. Loss-of-function on *PpMYB10.1* caused the absence of anthocyanin on peach skin. The color of peach fruit yellow vs. white fresh is regulated by another single gene, *PpCCD4*, localized on chromosome 1 [10]. These Mendelian traits show that *P. persica* is an excellent model woody species, also as a perennial crop, to explore the molecular mechanisms of some traits, especially on fruits.

Previous studies revealed that the trichome development on peach skin is also governed by a single gene, *PpMYB25*, at the *G* locus (glabrous locus) on chromosome 5 [8]. The glabrous trait of nectarines is recessive, designated "*g*". *PpMYB25* on the *G* locus, homologous to *GhMYB25*, is the master regulator of trichome formation in *P. persica* [32]. Thus, the trichome development appears to be conserved in cotton and *P. persica*. An insertion of transposon on exon3 of *PpMYB25* at the *G* locus impedes its transcription and leads to the loss of its function [26].

The fruits with and without trichomes are named as peach (*P. persica* L. Batsch) and nectarine (*P. persica* L. Batsch var. *nectarina*), respectively. Nectarine is classified as a subspecies of peach in botany [19]. The fuzz (trichomes) on peaches may lead to an undesirable mouthfeel, so breeding nectarines is a goal in various programs. Both peaches and nectarines are economically significant crops, and their annual economic output could reach to 25 million USD worldwide [25].

In this study, we performed genotyping and phenotyping of 295 *P. persica* accessions. To our surprise, we found one exception that was Maravilha Nectarine Mutant (MN). It was a peach in genotype possessing a putative functional *PpMYB25* gene sequence (*Gg*), but fruited as a nectarine in phenotype (no trichomes). The failure of trichome development under the presence of the functional master regulator *PpMYB25* gene sequence raises the following biological questions: Is trichome development not solely regulated by a single gene, *PpMYB25*? Or does a functional gene sequence not necessarily result in actual functionality in such accession? We thus conducted transcriptomic analyses on the fruits of this MN cultivar (*Gg*) together with that of other three cultivars (Tainung No.11-XingTao11 peach as *GG*, Tainung No.7-HongLing peach as *Gg*, Sunraycer nectarine as *gg*) to investigate the regulatory mechanisms of trichome development, especially on this MN cultivar.

Materials and methods

Plant materials and DNA extraction

A total of 295 accessions from the National Plant Genetic Resources Center (NPGRC) at Taiwan Agricultural Research Institute (TARI) were used for visual inspection of the present (peach) or absent trichomes (nectarine). The samples were collected at fruit set stage, where petals were shed, ovules developed into seeds and initial fruit organogenesis completed [32]. DNA of each accession was extracted using 0.1 g fresh leaves and the modified

CTAB (cetyltrimethyl ammonium bromide) procedure [9]. The concentration and quality of extracted DNA were measured using NanoDrop™ ND-1000 UV–Vis spectrophotometer (Thermo Scientific, Waltham, MA, USA) and gel electrophoresis, respectively.

Peach and nectarine genotyping

In addition to visual inspection of the trichomes on the skin of the peach fruit, the InDel G marker developed by Vendramin et al. [26] was screened in this study to discriminate the peach or nectarine genotypes. The sequence of primer set for Indel G marker are indelG-F (5'CTTGCACCTGAGTTCGATTCCG3'), indelG-1R (5'GGCTTCAATGGCAGAACAAGG3'), and indelG-2R (5'GCAGGTGGTGGAGATTCATTCAT3'). The polymerase chain reaction (PCR) formula was set up as follow: 10 µL Ampliqon Taq DNA polymerase 2× Master Mix RED with a final concentration of 1.5 mM $MgCl_2$ (Ampliqon, Denmark), 20 ng of template DNA, 0.2 µL of each 10 µM primers, and sterile ddH_2O to achieve a total volume of 20 µL. The PCR reaction was conducted using a ProFlex PCR System (Applied Biosystems, USA) with the following temperature profile: an initial hot start denaturation at 95 °C for 5 min, followed by 30 cycles of denaturation at 95 °C for 30 s, annealing at 60 °C for 30 s, and extension at 72 °C for 60 s. The final 5-min reaction was performed at 72 °C. Subsequently, the PCR products were analyzed through 2% (w/v) agarose gel electrophoresis in 1× TAE buffer, with an ethidium bromide (EtBr) staining.

RNA extraction and sequencing

Total RNA of the peach 'Tainung No.7-HongLing' (TN7) and 'Tainung No.11-XingTao' (TN11) with the *GG* and *Gg* genotype, and the nectarine 'Sunraycer' and 'Maravilha Nectarine Mutant' (MN); with *gg* and *Gg* genotype were extracted at the fruit set stage ($n = 5$ per accession) by RNeasy Plant Mini Kit (Qiagen, Germany) according to the manufacturer's instruction. Subsequently, the quality of isolated total RNA was assessed by Qsep400 Bio-Fragment Analyzer (BiOptic Inc., Taiwan). Library preparation was performed by TruSeq Stranded mRNA Library Prep Kit (Illumina, San Diego, CA, USA) following the manufacturer's instruction. Briefly, mRNA was purified from 1 µg of total RNA utilizing oligo (dT)-coupled magnetic beads. Following RNA fragmentation under elevated temperature, first-strand cDNA synthesis occurred using reverse transcriptase and random primers. Subsequently, double-strand cDNA was generated, and adaptors were ligated. The products underwent enrichment through PCR and purification using the AMPure XP system (Beckman Coulter, Beverly, USA). The quality of the cDNA libraries was assessed using the Qsep400 System (Bioptic Inc., Taiwan), and quantification was performed with a Qubit 2.0 Fluorometer (Thermo Scientific, Waltham, MA, USA). Finally, the qualified libraries were sequenced on an Illumina NovaSeq 6000 platform, generating 150 bp paired-end reads, by Genomics BioSci & Tech Co., New Taipei City, Taiwan.

Analysis of differential expression genes

In summary, the comprehensive analysis of transcriptomic data for identifying differentially expressed genes (DEGs) in peach and nectarine accessions was described in Figure S1. The raw reads obtained from the Illumina NovaSeq 6000 platform were processed using the FASTQ data pre-processing tool Fastp (version 0.23.2) to eliminate adapters and undergo quality filtering (FastpQC_paired.job). The peach genome annotation file and genetic information for chromosomes were sourced from the Joint Genomics Institute (https://phytozome-next.jgi.doe.gov/info/Ppersica_v2_1). Further refinement of the genomic annotation file involved the exon column was extracted and information of coding sequences (CDS) was added. For gene and transcript abundance quantification against a reference transcriptome, RSEM (version 1.2.31) coupled with Bowtie2 (version 2.5.1) alignment was performed. The analysis of differential expression genes utilized the DESeq2 package (version v1.34.0) within the R software environment (version 4.1.1). Analysis of DEGs were classified based on the criteria of an adjusted P-value < 0.05 and an absolute fold change > 1.5.

Principal component analysis

Principal component analysis (PCA) was performed by the DESeq2 package (version 1.34.0) within R software (version 4.1.1) and visualized with the ggplot2 package (version 3.4.2). First, read counts of each sample were imported and transferred into DESeqDataSet object with dispersion estimation and fitting model based on DESeq2. The DESeqDataSet was then transformed using the function of DESeq2 packag, varianceStabilizingTransformation. Finally, the plotPCA command was employed to perform PCA analysis and create a scatterplot, utilizing PC1 and PC2 as the X and Y axes.

Correlation of gene expression

Gene expression relationship analyses were conducted to test the association or correlation between paired samples using R software (version 4.2.1), in which the alternative hypothesis employed was"two-sided"and the method utilized was Pearson correlation. The target genes used for the calculation included *PpMYB25*, *PpMYB26*, and their upstream and downstream genes. Visualization of the correlation network illustrating the

relationships among *PpMYB25*, *PpMYB26*, and their respective upstream and downstream genes was generated using Cytoscape software (version 3.10.1).

Scanning electron microscopy

For sample preparation, 0.2 cm 2 pieces of fruit surfaces were cut from fruits of TN7, TN11, Sunraycer and MN. Each sample was mounted onto aluminum stub using double-sided sticky carbon tabs, was coated with gold in an Emitech K550X Sputter Coater to create electrical conductivity on the sample surface. The sample was imaged by the HITACHI SU3900 SEM in a high-vacuum mode operating at 5 kV and the working distance of 7–9 mm.

X-ray micro-tomography

In this study, the projection X-ray microscopy (PXM) at TPS31 A beamline of National Synchrotron Radiation Research Centre (NSRRC) in Taiwan was utilized to analyze the micro structure of the trichome for TN7, TN11, Sunraycer and MN. The energy of X-ray from synchrotron radiation of 20 keV was adopted by tuning a double crystal monochromator (DCM) to conduct 3-dimentional (3D) tomography of the specimen. The spatial resolution of image was 2.6 μm using 10X objective lens. The field of view was 8×3 mm^2 and the pixel number of image detector was 2560×2160. The temporal resolution was 10 min/tomography. The tomography was implemented by rotating the specimen azimuthally with a 0.25° interval through ± 90° range for 721 2D frames, and then reconstructed all 2D frames as a 3D tomography through an in-house developed software using filtered-back-projection algorithm. Finally, we use Amira 3D to analyze 3D internal structure of the sample.

Statistical analysis

The statistical significance of the differences between the abundance of expression genes among TN7, TN11, Sunraycer and MN were tested by Tukey's HSD test (P value < 0.05) using R software (version 4.1.1). The ANOVA (analysis of variance) for the mean abundance of expression genes was conducted following by pairwise comparison of mean abundance of expression genes by agricolae library (version 1.3–7).

Results

Fruit phenotypes of 295 accessions

The 295 accessions were breeding lines and cultivars collected from China, Japan, Taiwan, USA, Brazil, and South Africa. At least three biological replicates were used, and the morphology of trichome were recorded (Fig. 1A and Table S1). For each accession, the phenotypic results from three biological replicates were consistent. Among these 295 accessions, we observed total 262 accessions with the presence of trichome (i.e., peaches) and 33 accessions with the absence of trichome (i.e., nectarines) (Fig. 1A and Table S1).

Genotyping of the 295 *P. persica* accessions

The 295 accessions were also genotyped (Figure S2 and Table S1). *PpMYB25* located in the *G* locus of chromosome 5 (Fig. 1B). A recessive allele at the *G* locus (g) would exhibit a transposon integration, which cause the mutant of *PpMYB25*. In contrast, the dominant allele at the *G* locus would show the absence of such transposon (Fig. 1B). We adapted the two primer sets as IndelG_F/1R and IndelG_F/2R designed from previous studies [26] to examine the *G* locus (Fig. 1B). These two primer sets share the same forward primer (IndelG_F), but used different reverse primers (IndelG_1R or IndelG_2R). The primer sets spans across the exon 3 of *PpMYB25* coding region. Using all three primers in one PCR reaction (IndelG_F + IndelG_1R + IndelG_2R), we would be able to differentiate the genotypes into *GG*, *Gg*, and *gg*. In theory, the primer set of IndelG_F and IndelG_1R would generate a 197-bp PCR product for *g*, but the PCR reaction would be failed in *G*. The IndelG_F and IndelG_2R would generate a 6458 bp PCR product for *g* and a 941 bp product for *G*. Thus, a PCR reaction using all three primers together in *GG* would generate one PCR product as 941 bp, and that in *gg* would lead to two PCR products as 197 and 6458 bp. Practically, 6458 bp is too long for PCR, so *gg* would only results in one PCR product as 197 bp. Simply put, the PCR product of *G* using this primer set would lead to a bigger size of DNA fragment comparing to that of recessive *g*. Thus, the genotypes as *GG* and *gg* would both generate a single band on the gel after electrophoresis, while the single band from *gg* would be smaller due to the presence of the transposon. The genotype as *Gg* would then generate two bands each from *G* and *g*. Among the 295 accessions, 159 have the *GG* genotype, 104 have the *Gg* genotype, and 32 have the *gg* genotype. Although the genotype and phenotype are consistent in 294 out of 295 accessions, there is one exception: the Maravilha Nectarine mutant (MN), which exhibits the nectarine phenotype but carries the *Gg* genotype.

Transcriptomic analyses of the *Gg* accession lacking trichomes

To investigate molecular mechanisms causing the only exception (MN) of our genotype–phenotype screening, we performed transcriptomic analyses to explore the mechanisms involved in the failure of trichome formation under the genotype of functional *PpMYB25*. We also selected other three cultivars with different genotypes as

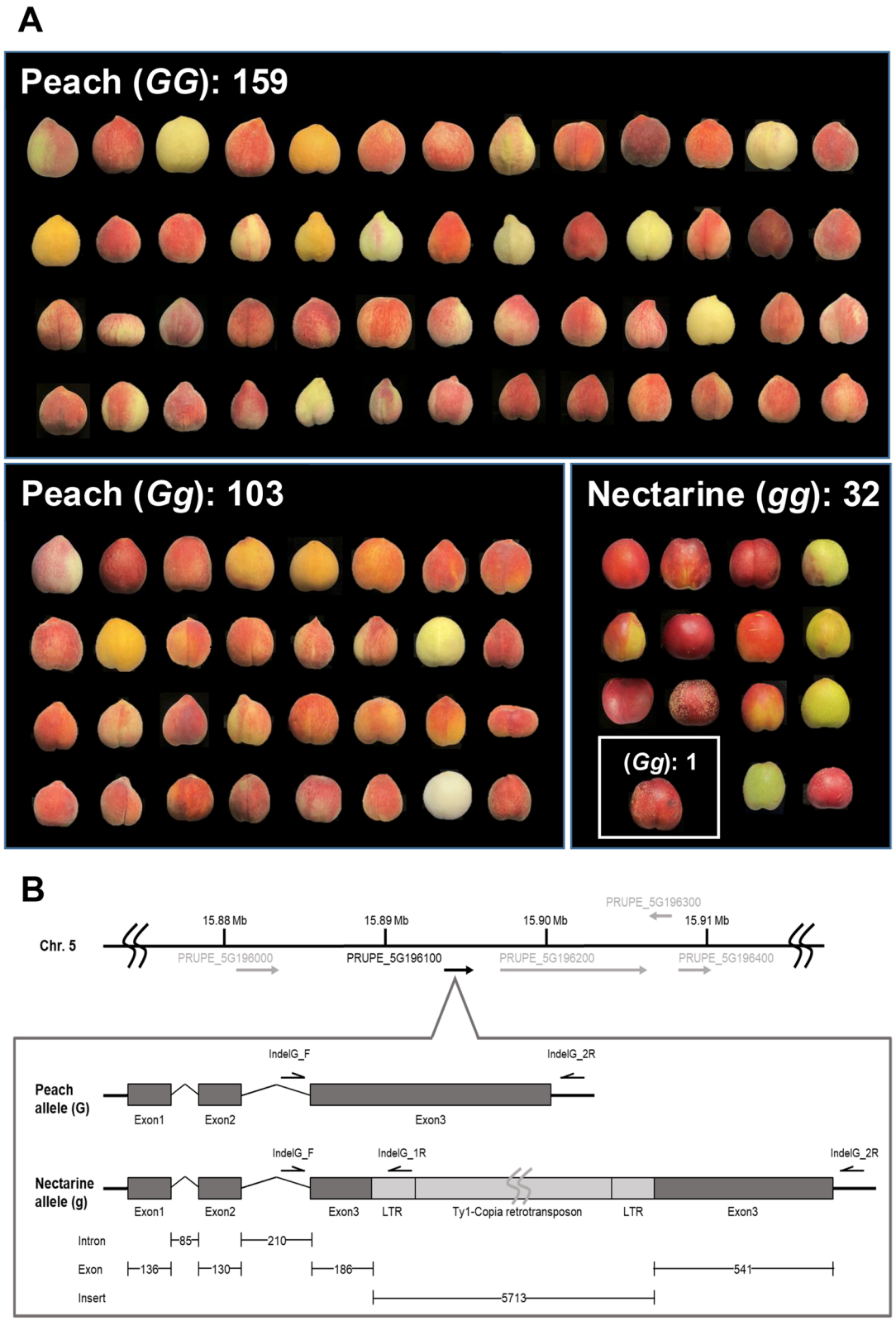

Fig. 1 Visual inspection and nectarine genotyping for the peach core collection. **A** Part of photographs, phenotype (peach or nectarine), genotype (*GG*, *Gg*, *gg*) and amounts of peach accessions at Taiwan Agricultural Research Institute (TARI). **B** Position of the main regulatory gene *PpMYB25* among *G* locus on chromosome 5 in peach along with the gene structures of the *G* allele (wild-type) and *g* allele (mutant). All genotyping results for 295 peach accessions were shown as Figure S2 and Table S1

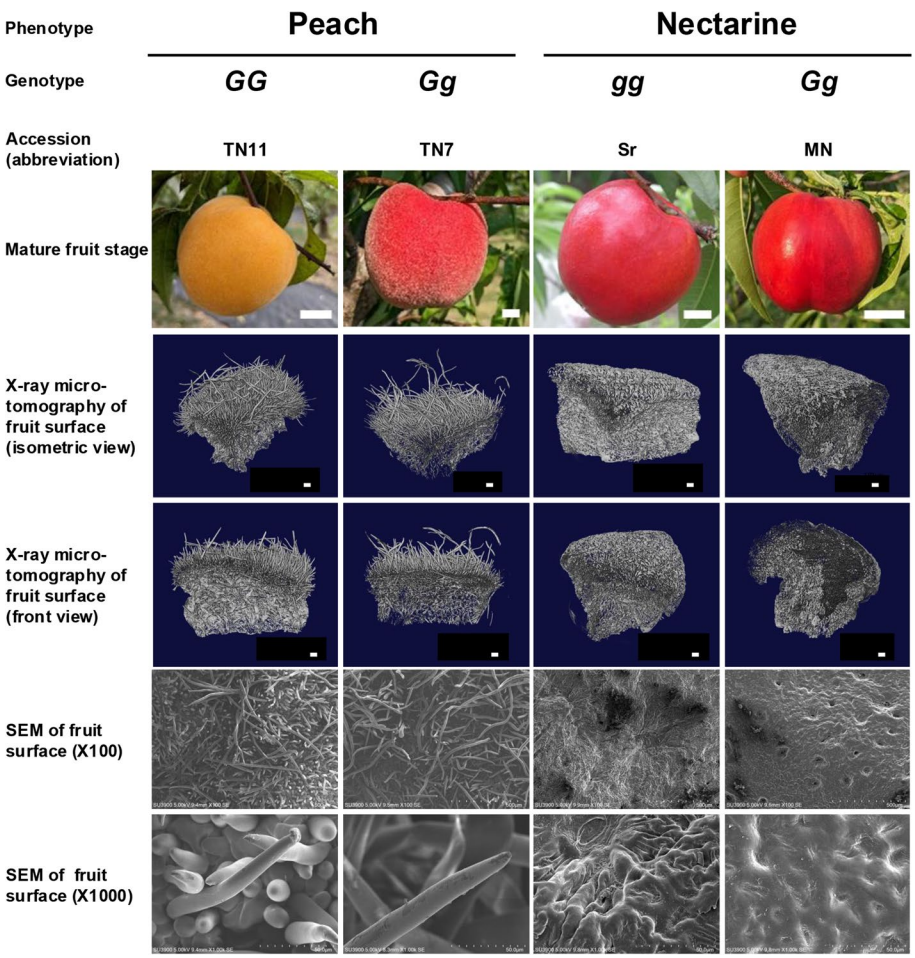

Fig. 2 Trichome morphology of peach and nectarine accessions. From top to bottom panels, this figure illustrates phenotypes, genotypes (white bar represents 2 cm), accession names, photographs of mature fruit, X-ray micro-tomography (CT) of fruit surfaces (isometric and front view, white bar represents 50 μm), and scanning electron microscopy (SEM) of fruit surfaces (the minimum unit of the scale are 500 and 50 μm for X100 and X1000, respectively) in four accessions. Peach accessions include the *GG* allele 'Tainung No.11-XingTao' (TN11), the *Gg* allele 'Tainung No.7-HongLin' (TN7) and the Nectarine accessions encompass the *gg* allele 'Sunraycer' (Sr), and the *Gg* allele 'Maravilha Nectarine Mutant' (MN)

the controls, including TN11 (*GG*), TN7 (*Gg*), and Sunraycer (*gg*) (Fig. 2). Thus, total four cultivars were used for comparative transcriptomic analyses: TN11 (*GG*, presence of trichome), TN7 (*Gg*, presence of trichome), Sunraycer (*gg*, absence of trichome), and MN (*Gg*, absence of trichome) (Fig. 2).

A total of 20 RNA samples, five biological replicates each for the four cultivars, were extracted, quantified, and used for the transcriptomic analyses. Our results showed high-quality total RNA samples were extracted using our pipeline, with the RNA Integrity Number (RIN) close to or equal to 10 (Figure S3A). These high-quality total RNA were then used to construct libraries for subsequent Illumina sequencing, and the libraries showed a qualified distribution with the sizes spanning mainly between 200 to 400 bp (Figure S3B). Read count and total sequencing output of 20 RNA samples were provided in Table S2.

Principal component analysis (PCA) was performed to compare the transcriptomic profiles among these samples (Fig. 3A). Two cultivars with the presence of trichomes (TN11 [*GG*] and TN7 [*Gg*]) located closely on the PCA plot, which demonstrate the highly consistency between their trichome phenotypes and their transcriptomic profiles. The other two cultivars with the absence of trichomes (Sunraycer and MN) separated from TN11 and TN7, showing potential different mechanisms on the regulation of trichome formation. However, Sunraycer and MN also separated from each other, and the results suggested two possible scenarios. First, the absence of trichome could be caused by different mechanism. Second, trichome formation is regulated by a small set of genes, so the transcriptomic difference could not explain the corresponding trichome phenotype.

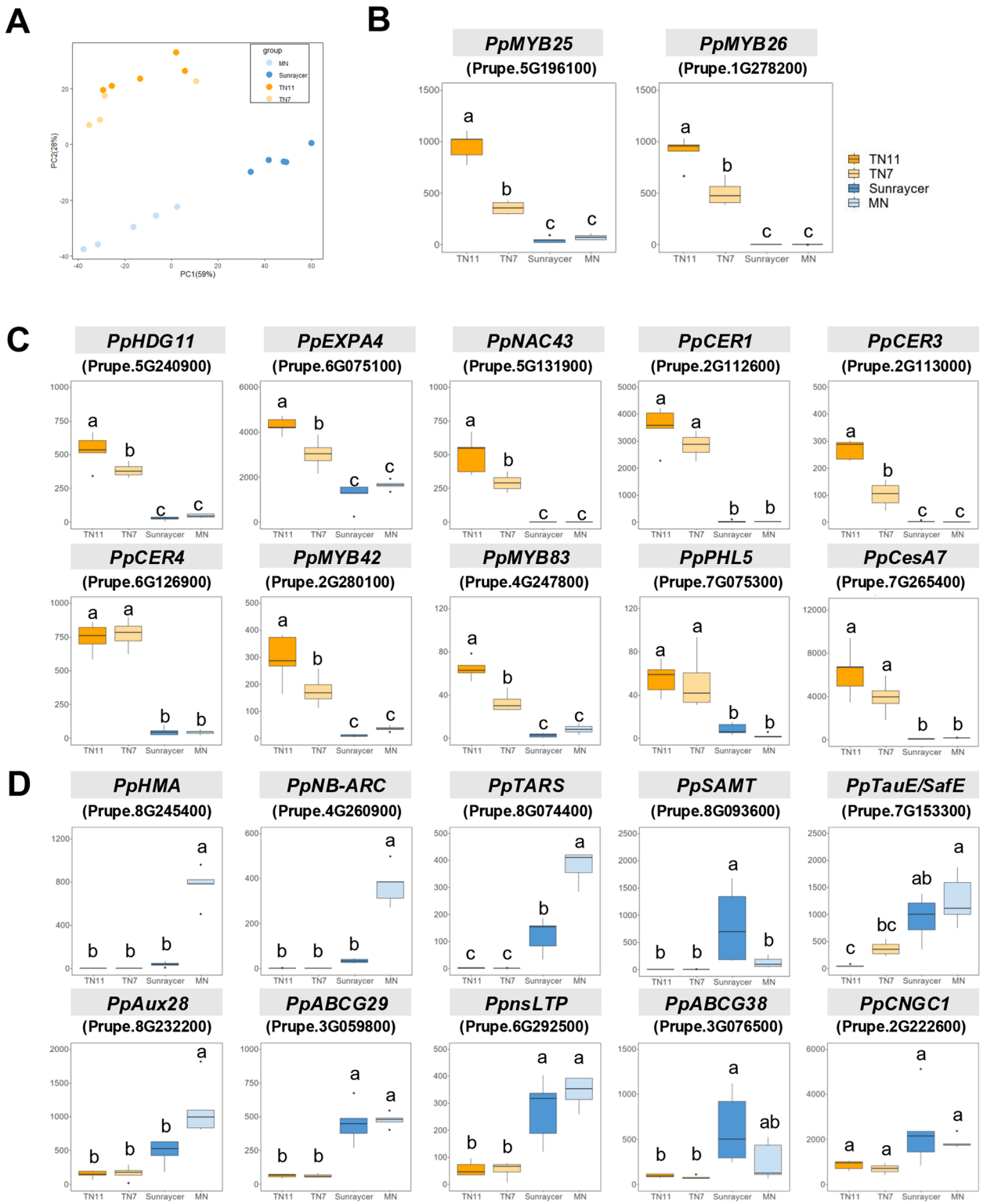

Fig. 3 Results of transcriptomic analysis of peach, the 'Tainung No.7-HongLin' (TN7) and 'Tainung No.11-XingTao' (TN11), and nectarine, the 'Sunraycer' (Sr) and 'Maravilha Nectarine Mutant' (MN). **A** Principal component analysis (PCA) based on read counts of the differentially expressed genes (DEGs). **B** Comparison of the mean abundance of the *PpMYB25* and *PpMYB26* transcripts. **C** Comparison of the mean abundance of the downstream genes that mediated by *PpMYB25* and *PpMYB26*. **D** Comparison of the mean abundance of the upstream genes that mediated by *PpMYB25* and *PpMYB26*. Means followed by the same letter within a column are not significantly different at the 0.05 level, as determined by Tukey's HSD test

Based on the previous results, the presence of trichome could be determined by a single gene, *PpMYB25* [26], so the current understanding prefers the possibility of the second scenario. We then extracted the transcriptomic information of *PpMYB25*, and examined its transcript abundance among different samples. In TN11, TN7 and Sunraycer, the transcript abundance of *PpMYB25* was consistent to the corresponding genotypes. The transcript of *PpMYB25* is basically undetectable in Sunraycer (*gg*). The transcript abundance of *PpMYB25* was higher in TN11 (*GG*) than that in TN7 (*Gg*), showing a dosage effect on the transcript abundance with the functional gene copy number (i.e., the number of the *G* allele) (Fig. 3B). Surprisingly, the transcript of *PpMYB25* in MN was also nearly undetectable, and the absence of *PpMYB25* transcript in MN is similar to that in Sunraycer. The lack of *PpMYB25* transcript in both MN and Sunraycer could explain their fruit phenotype without trichome.

We also examined the genes involved in the regulatory network of *PpMYB25*, including the downstream and upstream genes of *PpMYB25*. *PpMYB26* is one of the most well-known downstream genes of *PpMYB25* [32],Table S3), and we found that the relative transcript abundance of *PpMYB26* in the four cultivars is highly similar to that of *PpMYB25*, where the transcript in MN and Sunraycer is basically absent and that in TN11 was higher than in TN7 (Fig. 3B). The consistent pattern on transcript abundance between *PpMYB25* and *PpMYB26* further supported that trichome formation is determined by the regulatory network mediated by *PpMYB25*. In addition to *PpMYB26*, we further examined the transcript abundance of other downstream genes of *PpMYB25*, including *PpHDG11*, *PpEXPA4*, *PpNAC43*, *PpCER1*, *PpCER3*, *PpCER4*, *PpMYB42*, *PpMYB83*, *PpPHL5*, and *PpCESA7* (Fig. 3C). Again, the transcript abundance pattern of these genes among four cultivars is highly similar to that of *PpMYB25* and *PpMYB26*. Although *PpEXPA4* followed the similar pattern, its transcript abundance is not absent in MN and Sunraycer, which suggested that *PpMYB25* may not be the only upstream regulator of *PpEXPA4*.

In addition to the downstream genes of *PpMYB25*, we also investigated the transcript abundance of the upstream genes of *PpMYB25*, including *PpHMA*, *PpNB-ARC*, *PpTARS*, *PpSAMT*, *PpTauE*/*SafE*, *PpAux*/*IAA*, *PpABC transporter*, *PpnsLTP*, and *PpCNB binding protein* (Fig. 3C). We found that their transcript abundance was much lower in TN11 and TN7 than in MN and Sunraycer. Since *PpMYB25* expression was nearly absent in MN and Sunraycer, the plants might boost the abundance of the upstream regulators to try to enforce the execution of the *PpMYB25* pathway. Instead, *PpMYB25* functions effectively in TN11 and TN7, so the plants do not need to enhance the upstream regulators of *PpMYB25*.

Taken together of all of the transcript abundance patterns of *PpMYB25* and its upstream and downstream genes among the four cultivars (TN11, TN7, Sunraycer, and MN), the transcript abundance of *PpMYB25* is the determining factor on trichome formation. To further dissect the potential regulatory relationship between *PpMYB25* and its upstream and downstream genes, we performed correlation analyses among the genes involved in the *PpMYB25*-related regulatory network. In TN11 and TN7 with normal development of trichome, high correlations were shown among *PpMYB25*, *PpMYB26*, and their upstream and downstream genes (Fig. 4A). In contrast, these correlations were not detected in MN and Sunraycer without trichomes (Fig. 4B). Our results demonstrated that transcriptomic analyses on the investigation of the presence or absence of *PpMYB25* transcript is much more correlated to the trichome phenotypes instead of genomic analyses on functional gene coding regions.

Among the two cultivars with the presence of trichomes, the transcript abundance of *PpMYB25* is higher in TN11 than in TN7 due to different copies number of functional *PpMYB25* in TN11 (*GG*) and TN7 (*Gg*) (Fig. 3B). Since *PpMYB25* appears to be the master regulator of trichome formation, an intuitive idea would be raised that higher abundance of *PpMYB25* transcripts would lead to higher abundance phenotype on trichomes in terms of density or length. However, in our study, we found that the trichomes in TN11 (*GG*) are shorter than that in TN7 (*Gg*) (Fig. 2). In other words, *PpMYB25* only affected the presence or absence of trichome, but not the length.

Discussion

Among the 262 accessions with the presence of trichome (peaches), 159 were the *GG* genotype and 103 *Gg*. For the 33 accessions the absence of trichome (nectarines), 32 were *gg*, and 1 accession *Gg*. Overall, the results of 294 out of 295 accessions are consistent to previous studies [26]. Our results suggested that the phenotype of trichome in *P. persica* can be determined solely by the genotype of *PpMYB25* at the *G* locus of chromosome 5 with an extremely rare exception, the Maravilha Nectarine Mutant (MN) cultivar, regarded as a peach-to-nectarine mutant. The genotype of *G* locus from its wildtype, Maravilha, is also *Gg*. Some peach-to-nectarine mutants were also reported previously [5–7, 29]. Peach-to-nectarine mutants showed broad pleiotropic effects on fruit size, shape, and taste in addition to hairlessness [5, 30]. The genotypes of those previously reported

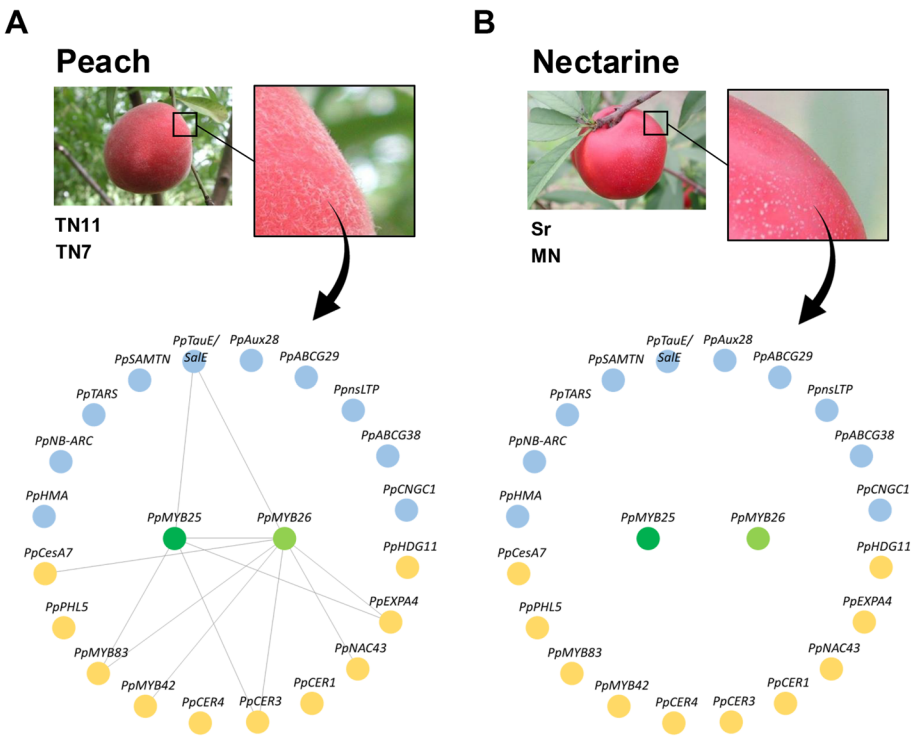

Fig. 4 The network diagram illustrates the statistically significant correlations ($P < 0.05$) involving *PpMYB25*, *PpMYB26*, and their upstream and downstream genes, as presented in Fig. 3. **A** The samples exhibiting normal trichome ['Tainung No.7-HongLin' (TN7) and 'Tainung No.11-XinTao' (TN11)] **B** The samples exhibiting lacking trichome ['Sunraycer' (Sr) and 'Maravilha Nectarine Mutant' (MN)]

peach-to-nectarine mutants still have not been reported, and the mechanisms involved in the failure of trichome formation in these mutants also remained unknown.

Other previous studies also suggested some cases with genotype *GG* or *Gg* but exhibiting as nectarine. In addition to the transposon insertion on exon 3, some *P. persica* cultivars possessed transposon insertion on the exon 2 of *PpMYB25*, and the insertion also led to the loss of function [22]. Another previous study performed a large-scale screening on the *P. persica* cultivars without trichomes on the fruits (named as hairlessness phenotype), but found the absence of transposon insertion on *PpMYB25* [18]. Instead of the loss of function caused by transposon insertion, such study discovered several single nucleotide polymorphisms (SNPs) on *PpMYB25*, which also abolished its function [22]. Thus, numerous studies have shown that trichome development in *P. persica* is controlled by a single gene, *PpMYB25*. However, comparing to the reference genome, the *G* of MN does not possess any of the SNPs (Figure S4), which suggests another type of regulation beyond the changes on genome sequences. Different types of regulations could result in such loss-of-function phenomenon, including epigenetic regulation to adjust the transcript abundance or post-transcriptional/translational regulation to alter RNA or protein structures.

We conducted comparative analyses for the mechanisms that lead to the absence of trichome development. Total 118 accessions were collected for the comparative analyses, and these accessions includes 85 accessions from previous studies and 33 accessions from our study (Figure S5). Almost all genotypes (116 accessions) showed a T-DNA insertion (98.31%), and one accession exhibits SNPs (0.85%). Only one accession—the MN accession—exhibits the trichome-absent trait without any associated T-DNA insertion or SNPs. This finding suggests that the mechanism we identified is exceptionally rare and may represent a novel or previously overlooked pathway underlying the trichome-absent phenotype.

MN is a cultivar derived from sport mutation. This type of mutation is a common phenomenon among fruit tree, such as apple and citrus [3]. In apple, sport mutation is one of the main avenues for breeders to generate new cultivars with diverse on ripening time [14], or fruit skin colors [28]. The different phenotypes caused by sport mutation in apple were found to lead to alternative genetic or epigenetic regulation [28]. In our study, we identified another case of sport mutation in peach, which might be regulated by epigenetics.

Previous studies have reported that trichome formation in an eudicot weed species, *Mimulus guttatus*, is regulated through epigenetic manners. In different regions, *M. guttatus* exhibited different trichome densities on leaves. One of the most distinct trait among there regions is the frequency of herbivore feeding. Through a common-garden strategy, that research team applied various mechanical stress on the leaves. Upon the treatment of the mechanical stress, they found the high correlation of trichome density with the intensity of mechanical stress, and such phenomenon could last for at least two generations [20]. In our study, we found that trichome formation could also be regulated through epigenetic manners on *PpMYB25* in *P. persica*. With the functional coding region of *PpMYB25* in MN cultivar, the plants could turn off the transcription of *PpMYB25* to abolish its function. Core eudicots is composed of two representative evolutionary clades, rosids and asterids. *M. guttatus* and *P. persica* respectively belong to asterids and rosids. Since trichome formation was found to be regulated by epigenetics manners in both *M. guttatus* (asterids) and *P. persica* (rosids), the epigenetic regulation of trichome formation appears to be conserved throughout the whole core eudicots.

Conclusions

Trichomes in peach represent specialized structures that play pivotal roles for the protection against both biotic and abiotic stressors. Genetically, the development of trichomes in peach is primarily regulated by a single gene, *PpMYB25*, situated on the *G* locus. *G* and *g* respectively represent a functional and a knockout locus. Through the examination of trichome formation across 295 accessions, we identified a specific accession (MN) that harbored a putative functional *PpMYB25* gene sequence (*Gg*) but exhibited a nectarine

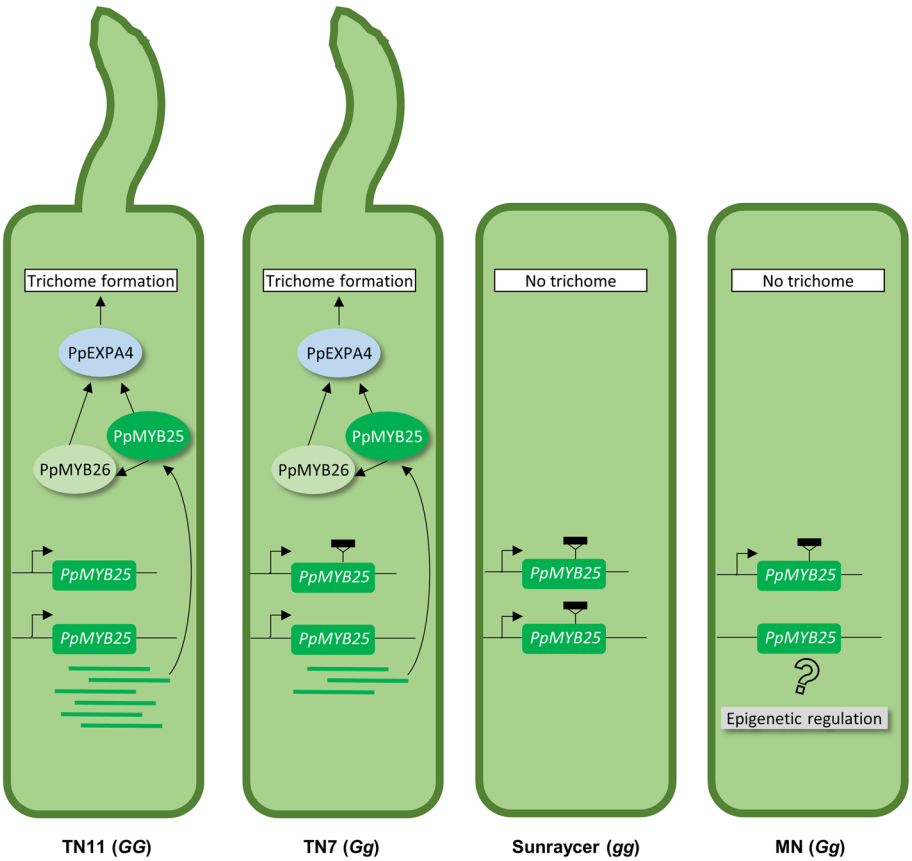

Fig. 5 Schematic regulatory models of trichome formation models for peach and nectarine accessions. Regulatory control of trichrome formation at transcriptomic level for peach, the 'Tainung No.7-HongLin' (TN7) and 'Tainung No.11-XingTao' (TN11), and nectarine, the 'Sunraycer' (Sr) and 'Maravilha Nectarine Mutant' (MN) were illustrated. The TN7 with *GG* genotype expressed functional *PpMYB25* manifested normal trichome formation. Ever though insertion of transposon (black rectangle) in one chromosome of the TN11 resulted in loss of function of the *PpMYB25*, expression of the remaining functional *PpMYB25* led to normal trichome formation. For Sunraycer with *gg* genotype, both *PpMYB25* possessed transposon insertion and contributed to no expression of *PpMYB25*. Putative epigenetic regulation was proposed to block the expression of the functional *PpMYB25* for the MN with *Gg* genotype, therefore no trichome formation was observed

phenotype as the absence of trichomes. Transcriptomic analyses were used to explore the mechanisms of trichome formation in MN, and other three accessions were used as control: TN11 (*GG*, peach), TN7 (*Gg*, peach), and Sunraycer (*gg*, nectarine). The presence and absence of *PpMYB25* transcript were consistent to the trichome phenotypes in all accessions that *PpMYB25* is not expressed in neither Sunraycer and MN (Figs. 3, and 5). In addition to the absence of *PpMYB25* transcript, correlation network analyses showed that *PpMYB25*-mediated regulatory network was also abolished in Sunraycer and MN (Figs. 4 and 5). Our results demonstrated an alternative regulatory mechanism beyond genetic regulation on trichome formation, which is highly likely to be derived from epigenetic regulation (Fig. 5).

Supplementary Information

The online version contains supplementary material available at https://doi.org/10.1186/s12870-025-06622-7.

Supplementary Material 1

Acknowledgements
The authors would like to thank Mr. Chien-Yu Lee, Dr. Bo-Yi Chen, Mr. Ying-Shuo Tseng, Mr. Shih-Ting Lo, and Dr. Hsiu-Chien Chan of NSRRC for their help in PXM setup and image execution. The assistance provided by Mei-Jung Tseng and Wen-Shiou Deng of Applied Zoology Division of TARI for the SEM imaging also are acknowledged gratefully.

Authors' contribution
C.C.H.: Resources, Writing—Original Draft, Visualization, Methodology, Conceptualization. H.W.C.: Validation, Investigation, Data Curation, Writing—Original Draft, Visualization. J.W.A.H.: Formal Analysis, Investigation, Data Curation. Y.C.L: Validation, Investigation, Data Curation, Visualization. Y.P.L: Validation, Investigation, Data Curation. C.C.: Writing—Review & Editing. Y.F.S.: Investigation, Data Curation. G.C.Y.: Investigation, Data Curation. T.L.M.: Software, Data Curation, Visualization. Y.C.J.L: Writing—Original Draft, Writing—Review & Editing, Supervision, Methodology, Conceptualization. Y.K.T: Project Administration, Writing—Original Draft, Supervision, Methodology, Conceptualization.

Funding
This study was financially supported by the project # 112YIB040001 'Studies on international exchange and extension strategies of agricultural- Study on Genetic Background and Molecular Marker Assistant Selection in Peach Germplasm' and the project # 113 AS-1.3.2-AS-29 'Transcriptomics analysis to reveal trichome developmental mechanisms in peach and nectarine'. Both projects were funded by the Ministry of Agriculture (MOA), Taiwan. T.L.M. was supported by NSTC (112–2221-E-002–191-MY3) and Yushan Fellow Program by the Ministry of Education (MOE-112-YSFAG-0003–002-P1).

Data availability
The datasets generated and analyzed in this study are available in the GEO repository under accession number GSE291534.

Declarations

Ethics approval and consent to participate
Not applicable.

Consent for publication
Not applicable.

Competing interests
The authors declare no competing interests.

Received: 28 February 2025 Accepted: 25 April 2025
Published online: 10 May 2025

References

1. Abbott A, Georgi L, Yvergniaux D, Wang Y, Blenda A, Reighard G, Inigo M, Sosinski B. Peach: the model genome for Rosaceae. Acta Hortic. 2002;575:145–55. https://doi.org/10.17660/ActaHortic.2002.575.14.
2. Arús P, Verde I, Sosinski B, Zhebentyayeva T, Abbott AG. The peach genome. Tree Genet. Genomes. 2012;8:531–47. https://doi.org/10.1007/s11295-012-0493-8.
3. Ban JC, Jung JH. Somatic mutations in fruit trees: causes, detection methods, and molecular mechanisms. Plants. 2023;12:1316. https://doi.org/10.3390/plants12061316.
4. Busta L, Hegebarth D, Kroc E, Jetter R. Changes in cuticular wax coverage and composition on developing *Arabidopsis* leaves are influenced by wax biosynthesis gene expression levels and trichome density. Planta. 2017;245:297–311. https://doi.org/10.1007/s00425-016-2603-6.
5. Chen C, Bai J, Okie WR, Plotto A. Comparison of fruit characters and volatile components in peach-to-nectarine mutants. Euphytica. 2016;209:409–18. https://doi.org/10.1007/s10681-016-1648-8.
6. Dagar A, Weksler A, Friedman H, Ogundiwin EA, Crisosto CH, Ahmad R, Lurie S. Comparing ripening and storage characteristics of 'Oded' peach and its nectarine mutant 'Yuval', Postharvest Biol. Technol. 2011;60:1–6. https://doi.org/10.1016/j.postharvbio.2010.11.002.
7. Dagar A, Puig CP, Ibanez CM, Ziliotto F, Bonghi C, Crisosto CH, Friedman H, Lurie S, Granell A. Comparative transcript profiling of a peach and its nectarine mutant at harvest reveals differences in gene expression related to storability, Tree Genet. Genomes. 2012;9:223–35. https://doi.org/10.1007/s11295-012-0549-9.
8. Dirlewanger E, Cosson P, Boudehri K, Renaud C, Capdeville G, Tauzin Y, Laigret F, Moing A. Development of a second-generation genetic linkage map for peach [*Prunus persica* (L.) Batsch] and characterization of morphological traits affecting flower and fruit Tree Genet. Genomes. 2006;3:1–13. https://doi.org/10.1007/s11295-006-0053-1.
9. Doyle JJ, Doyle JL. A rapid DNA isolation procedure for small quantities of fresh leaf tissue. Phytochem Bull. 1987;19:11–5.
10. Falchi R, Vendramin E, Zanon L, Scalabrin S, Cipriani G, Verde I, Vizzotto G, Morgante M. Three distinct mutational mechanisms acting on a single gene underpin the origin of yellow flesh in peach. Plant J. 2013;76:175–87. https://doi.org/10.1111/tpj.12283.
11. Hauser M. Molecular basis of natural variation and environmental control of trichome patterning. Front Plant Sci. 2014;5:99452. https://doi.org/10.3389/fpls.2014.00320.
12. Hegebarth D, Buschhaus C, Wu M, Bird D, Jetter R. The composition of surface wax on trichomes of *Arabidopsis thaliana* differs from wax on other epidermal cells. Plant J. 2016;88:762–74. https://doi.org/10.1111/tpj.1329.
13. Ishida T, Kurata T, Okada K, Wada T. A genetic regulatory network in the development of trichomes and root hairs. Annu Rev Plant Biol. 2008;59:365–86. https://doi.org/10.1146/annurev.arplant.59.032607.092949.
14. Jahed KR, Hirst PM. Fruit growth and development in apple: a molecular, genomics and epigenetics perspective. Front Plant Sci. 2023;14:1122397. https://doi.org/10.3389/fpls.2023.1122397.
15. Jakoby MJ, Falkenhan D, Mader MT, Brininstool G, Wischnitzki E, Platz N, Hudson A, Hülskamp M, Larkin J, Schnittger A. Transcriptional profiling of mature *Arabidopsis* trichomes reveals that NOECK encodes the MIXTA-like transcriptional regulator MYB106. Plant Physiol. 2008;148:1583–602. https://doi.org/10.1104/pp.108.126979.
16. Konrad W, Roth-Nebelsick A, Kessel B, Miranda T, Ebner M, Schott R, Nebelsick JH. The impact of raindrops on *Salvinia molesta* leaves: effects of trichomes and elasticity. J R Soc Interface. 2021;18:1–14. https://doi.org/10.1098/rsif.2021.0676.
17. Koudounas K, Manioudaki ME, Kourti A, Banilas G, Hatzopoulos P. Transcriptional profiling unravels potential metabolic activities of the olive leaf non-glandular trichome. Front Plant Sci. 2015;6:149895. https://doi.org/10.3389/fpls.2015.00633.

18. Lu Z, Pan L, Wei B, Niu L, Cui G, Wang L, Zeng W, Wang Z. Fine mapping of the gene controlling the fruit skin hairiness of *Prunus persica* and its uses for mas in progenies. Plants. 2021;10:1433. https://doi.org/10.3390/plants10071433.
19. Özelkök S, Ertan Ü, Kaynas K. Maturity and ripening concepts on nectarines. A case study on "NECTARED-6" and "INDEPENDENCE." Acta Hortic. 1997;441:287–94. https://doi.org/10.17660/ActaHortic.1997.441.39.
20. Scoville AG, Barnett LL, Bodbyl-Roels S, Kelly JK, Hileman LC. Differential regulation of a MYB transcription factor is correlated with transgenerational epigenetic inheritance of trichome density in *Mimulus guttatus*. New Phytol. 2011;191:251. https://doi.org/10.1111/j.1469-8137.2011.03656.x.
21. Swarbreck D, Wilks C, Lamesch P, Berardini TZ, Garcia-Hernandez M, Foerster H, Li D, Meyer T, Muller R, Ploetz L, Radenbaugh A, Singh S, Swing V, Tissier C, Zhang P, Huala E. The Arabidopsis Information Resource (TAIR): gene structure and function annotation. Nucleic Acids Res. 2008;36:D1009–14. https://doi.org/10.1093/nar/gkm965.
22. Tan Q, Li S, Zhang Y, Chen M, Wen B, Jiang S, Chen X, Fu X, Li D, Wu H, Wang Y, Xiao W, Li L. Chromosome-level genome assemblies of five *Prunus* species and genome-wide association studies for key agronomic traits in peach. Hortic Res. 2021;8:1–18. https://doi.org/10.1038/s41438-021-00648-2.
23. Tuan PA, Bai S, Yaegaki H, Tamura T, Hihara S, Moriguchi T, Oda K. The crucial role of *PpMYB10.1* in anthocyanin accumulation in peach and relationships between its allelic type and skin color phenotype. BMC Plant Biol. 2015;15:280. https://doi.org/10.1186/s12870-015-0664-5.
24. Tuskan GA, DiFazio S, Jansson S, Bohlmann J, Grigoriev I, Hellsten U, Putnam N, Ralph S, Rombauts S, Salamov A, Schein J, Sterck L, Aerts A, Bhalerao RR, Bhalerao RP, Blaudez D, Boerjan W, Brun A, Brunner A, Busov V, Campbell M, Carlson J, Chalot M, Chapman J, Chen G, Cooper D, Coutinho PM, Couturier J, Covert S, Cronk Q, Cunningham R, Davis J, Degroeve S, Déjardin A, dePamphilis C, Detter J, Dirks B, Dubchak I, Duplessis S, Ehlting J, Ellis B, Gendler K, Goodstein D, Gribskov M, Grimwood J, Groover A, Gunter L, Hamberger B, Heinze B, Helariutta Y, Henrissat B, Holligan D, Holt R, Huang W, Islam-Faridi N, Jones S, Jones-Rhoades M, Jorgensen R, Joshi C, Kangasjärvi J, Karlsson J, Kelleher C, Kirkpatrick R, Kirst M, Kohler A, Kalluri U, Larimer F, Leebens-Mack J, Leplé J, LoCascio P, Lou Y, Lucas S, Martin F, Montanini B, Napoli C, Nelson DR, Nelson C, Nieminen K, Nilsson O, Pereda V, Peter G, Philippe R, Pilate G, Poliakov A, Razumovskaya J, Richardson P, Rinaldi C, Ritland K, Rouzé P, Ryaboy D, Schmutz J, Schrader J, Segerman B, Shin H, Siddiqui A, Sterky F, Terry A, Tsai C, Uberbacher E, Unneberg P, Vahala J, Wall K, Wessler S, Yang G, Yin T, Douglas C, Marra M, Sandberg G, Van de Peer Y, Rokhsar D. The genome of black cottonwood, *Populus trichocarpa* (Torr. & Gray). Science. 2006;313:1596–604. https://doi.org/10.1126/science.1128691.
25. USDA-FAS, 2023. Stone Fruit, USDA-FAS annual report. https://apps.fas.usda.gov/psdonline/circulars/StoneFruit.pdf (accessed 10 January, 2024,)
26. Vendramin E, Pea G, Dondini L, Pacheco I, Dettori MT, Gazza L, Scalabrin S, Strozzi F, Tartarini S, Bassi D, Verde I, Rossini L. A unique mutation in a MYB gene cosegregates with the nectarine phenotype in peach. PLoS ONE. 2014;9:e112032. https://doi.org/10.1371/journal.pone.0090574.
27. Verde I, Jenkins J, Dondini L, Micali S, Pagliarani G, Vendramin E, Paris R, Aramini V, Gazza L, Rossini L, Bassi D, Troggio M, Shu S, Grimwood J, Tartarini S, Dettori MT, Schmutz J. The Peach v2.0 release: high-resolution linkage mapping and deep resequencing improve chromosome-scale assembly and contiguity. BMC Genom. 2017;18:225. https://doi.org/10.1186/s12864-017-3606-9.
28. Wang W, Celton JM, Buck-Sorlin G, Balzergue S, Bucher E, Laurens F. Skin color in apple fruit (*Malus* × *domestica*): Genetic and epigenetic insights. Epigenomes. 2020;4:13. https://doi.org/10.3390/epigenomes4030013.
29. Wen IC, Koch KE, Sherman WB. Comparing fruit and tree characteristics of two peaches and their nectarine mutants. J Am Soc Hortic Sci. 1995;120:101–6. https://doi.org/10.21273/JASHS.120.1.101.
30. Wen IC, Sherman WB, Koch KE. Heritable pleiotropic effects of the nectarine mutant from peach. J Am Soc Hortic Sci. 1995;120:721–5. https://doi.org/10.21273/JASHS.120.5.721.
31. Yan A, Pan J, An L, Gan Y, Feng H. The responses of trichome mutants to enhanced ultraviolet-B radiation in *Arabidopsis thaliana*. J. Photochem. Photobiol. B, Biol. 2012;113:29–35. https://doi.org/10.1016/j.jphotobiol.2012.04.011.
32. Yang Q, Yang X, Wang L, Zheng B, Cai Y, Ogutu CO, Zhao L, Peng Q, Liao L, Zhao Y, Zhou H, Han Y. Two R2R3-MYB genes cooperatively control trichome development and cuticular wax biosynthesis in *Prunus persica*. New Phytol. 2022;234:179–96. https://doi.org/10.1111/nph.17965.
33. Yuan Y, Xu X, Luo Y, Gong Z, Hu X, Wu M, Liu Y, Yan F, Zhang X, Zhang W, Tang Y, Feng B, Li Z, Jiang CZ, Deng W. R2R3 MYB-dependent auxin signalling regulates trichome formation, and increased trichome density confers spider mite tolerance on tomato. Plant Biotechnol J. 2021;19:138–52. https://doi.org/10.1111/pbi.13448.
34. Zhou H, Ma R, Gao L, Zhang J, Zhang A, Zhang X, Ren F, Zhang W, Liao L, Yang Q, Xu S, Otieno Ogutu C, Zhao J, Yu M, Jiang Q, Korban SS, Han Y. A 1.7-Mb chromosomal inversion downstream of a *PpOFP1* gene is responsible for flat fruit shape in peach. Plant Biotechnol J. 2021;19:192–205. https://doi.org/10.1111/pbi.13455.
35. Zhu Q, Stiller W, Moncuquet P, Gordon S, Yuan Y, Barnes S, Wilson I. Genetic mapping and transcriptomic characterization of a new fuzzless-tufted cottonseed mutant. G3 (Bethesda). 2021;11:1–14. https://doi.org/10.1093/g3journal/jkaa042.
36. Zhu QH, Yuan Y, Stiller W, Jia Y, Wang P, Pan Z, Du X, Llewellyn D, Wilson I. Genetic dissection of the fuzzless seed trait in *Gossypium barbadense*. J Exp Bot. 2018;69:997–1009. https://doi.org/10.1093/jxb/erx459.

Publisher's Note